JOURNAL OF MATERIALS SCIENCE 31 (1996) 6263–6267

Rare-earth doped zirconia fibres by sol–gel processing

M. K. NASKAR, D. GANGULI
Sol-Gel Laboratory, Central Glass and Ceramic Research Institute, Calcutta 700 032, India

Polycrystalline zirconia fibres, doped with 2–8 mol % of oxides of trivalent lanthanum, praseodymium, neodymium, samarium, gadolinium, and dysprosium (in decreasing cation size), were prepared by spinning of acetate-derived sols and baking the gel fibres thus obtained at 900 – 1300 °C for 1 h. The larger sized dopants lanthanum, praseodymium and neodymium (Group A) gave rise to tetragonal zirconia, with or without cubic zirconia, at 900 °C which converted partly or fully to monoclinic zirconia, in certain cases accompanied by a cubic zirconate phase at higher temperatures. The smaller sized dopants samarium, gadolinium and dysprosium (Group B) generated only tetragonal or cubic, or both polymorphs of zirconia, depending on the cation type, concentration and temperature. This "stabilization" of higher symmetry polymorphs with Group B dopants was associated with relatively large crystallite size (especially when calcined at 1300 °C). The maximum tensile strength values of usable fibres calcined at 1300 °C were found to decrease with increasing size in dopant dysprosium > gadolinium > samarium > neodymium, praseodymium, lanthanum = 0). Although all the dopant cations were larger in size than Zr^{4+} (in the same oxygen coordination), the relative closeness in size of Group B cations with Zr^{4+} was considered to be the reason behind the obtained differences in properties.

1. Introduction

Zirconia fibres have gained importance in recent times for application in high-temperature insulation, and lately, ceramic–ceramic composites [1, 2]. Different variants of the sol–gel processing technique have been used recently to prepare partially and fully stabilized zirconia fibres. The dopants commonly used were magnesium, calcium and yttrium [3–7].

While some rare-earth (RE) ions have been used in the preparation of partially and fully stabilized zirconia powders and ceramics [8, 9], little systematic information is available on the effect of RE ions on the properties of zirconia fibres; the main controlling factor is, of course, the size of the RE ion with respect to that of zirconium with similar oxygen co-ordination.

Therefore, different percentages (2–8 mol % oxide) of RE ions (lanthanum, praseodymium, neodymium, samarium, gadolinium and dysprosium, in decreasing cation size), were used for the preparation of doped zirconia fibres by sol spinning and calcination of gel fibres, and their evaluation.

2. Experimental procedure

2.1. Sol and fibre preparation

A precipitate of hydrated zirconia was obtained by the action of 1:1 vol/vol aqueous ammonia solution (25 wt %, pure, E. Merck, India) on a solution of zirconium oxychloride octahydrate (ZrO_2, 36.5%, Indian Rare Earths Ltd) in deionized water. The precipitate was peptized with glacial acetic acid (99.8%, AnalaR, BDH, India) under stirring at 60–70 °C. The mother sol thus obtained (1.47 M equivalent ZrO_2 content) was divided into parts, and in each part an aqueous nitrate solution of one of the cations lanthanum, praseodymium, neodymium, samarium, gadolinium, or dysprosium in 2, 5 and 8 equivalent oxide mol %, was mixed under stirring. Hydrogen peroxide (molar ratio $H_2O_2:ZrO_2 = 5:1$) was added dropwise in these sols during stirring. The sols were kept at 5 °C for 24 h. The eighteen sols thus prepared were aged at 70–80 °C for different times to obtain spinnability (checked by hand-drawing of the fibres). The sols thus prepared were spun in a laboratory spinneret and the gel fibres gathered from a receptacle drum.

The gel fibres were oven-dried at 200 °C for 1 h and finally calcined at 900, 1100 and 1300 °C, all for 1 h, with a heating rate of 1 °C min^{-1} and a cooling rate of 5 °C min^{-1} down to 200 °C, followed by furnace cooling. The weight loss was 48–50% in all cases.

2.2. Characterization of fibres

Crystal-phase developments in the gel fibres after calcination were examined by X-ray diffractometry (Philips PW-1730 X-ray unit). The crystallite sizes of the different ZrO_2 (solid solution) phases were calculated using Scherer's formula [10]

$$D = (0.9\lambda)/\beta\cos\theta \qquad (1)$$

where λ is the wavelength of the radiation (CuK_α), θ the diffraction angle and β the corrected half-width of

0022–2461 © *1996 Chapman & Hall*

the strongest diffraction peak of the respective phase. According to the method of Klug and Alexander [10]

$$\beta = (B^2 - b^2)^{1/2} \qquad (2)$$

where B and b are the observed line-widths at half-intensity of crystalline ZrO_2 and α-quartz (in this case), respectively. The peaks (θ in Equation 1) used for the measurement of D were $(11\bar{1})$ for monoclinic (m), (1 1 1) for tetragonal/cubic (t/c), (1 1 1) for $cNd_{0.25}Zr_{0.75}O_{1.875}$ (N) and (2 2 2) for $cLa_2Zr_2O_7$(L) or $cPr_2Zr_2O_7$ (P). Lattice strain was calculated from the equation [11]

$$\beta\cos\theta/\lambda = 1/D + \eta\sin\theta/\lambda \qquad (3)$$

The tensile strength of the fibres was measured on an improvized apparatus as used by Kamiya *et al.* [6]. The measurement followed the relationship [12]

$$\text{tensile strength} = \frac{\text{fracture load}}{\text{fibre cross-sectional area}} \qquad (4)$$

The grain sizes in calcined fibres were measured from scanning electron micrographs by the line-intercept method [13].

3. Results and discussion

3.1. Crystalline phases

The development of different crystalline phases as a function of dopant concentration and temperature of calcination of the gel fibres is shown in Table I where the cations have been arranged according to decreasing size to emphasize the control of size on phase development. The salient features of these results are summarized below.

(i) After calcination at 900 °C, fibres with 2 mol % dopant yielded t-ZrO_2 as the only crystalline phase; with increase in dopant concentration, c-ZrO_2 formed (5 mol %) and apparently increased in proportion (8 mol %).

(ii) On calcination at 1100 °C, fibres with 2 mol % lanthanum oxide and praseodymium oxide showed the formation of the m-phase along with t-ZrO_2. The other dopants (2 mol %) yielded only t-ZrO_2. With increasing dopant concentration, the t-phase was accompanied by the cubic $Ln_2Zr_2O_7$-type zirconate phase in the case of lanthanum, while for the others, the additional phase was c-ZrO_2. Zirconate phases are also known for all the other cations of Table I [8, 14, 15]; however, up to 1100 °C calcination, none of these phases could be detected.

(iii) Calcination at 1300 °C yielded only the m-phase for 2 mol % doping with lanthanum and praseodymium; for neodymium, the m-phase was accompanied by the t-phase. For the rest, only the t-phase was obtained. When the dopant content was increased, the zirconate phases crystallized in the case of lanthanum, praseodymium and neodymium in addition to the m-phase or a mixture of (m + t)-ZrO_2. For samarium, gadolinium and dysprosium, no zirconate phase was formed, and the product was t-ZrO_2. For the two smallest cations, cubic zirconia solid solution could be obtained as the single phase with the highest level of doping at 1100 and 1300 °C, indicating full stabilization.

TABLE I Phase identification of rare-earth oxide-doped zirconia fibres at various temperatures by XRD

Composition (mol %)	Phase(s) at		
	900 °C	1100 °C	1300 °C
$98ZrO_2$ $2La_2O_3$	t	t + m	m
$95ZrO_2$ $5La_2O_3$	t + c (small)	t + L (small)	m + L
$92ZrO_2$ $8La_2O_3$	c + t	t + L	L + m
$98ZrO_2$ $2Pr_2O_3$	t	t + m	m
$95ZrO_2$ $5Pr_2O_3$	t + c	t + c	m + P + t (small)
$92ZrO_2$ $8Pr_2O_3$	c + t	c + t	P + m
$98ZrO_2$ $2Nd_2O_3$	t	t	m + t
$95ZrO_2$ $5Nd_2O_3$	t + c	t + c	t + N
$92ZrO_2$ $8Nd_2O_3$	c + t	c + t (small)	N + t
$98ZrO_2$ $2Sm_2O_3$	t	t	t
$95ZrO_2$ $5Sm_2O_3$	t + c	t + c	t + c
$92ZrO_2$ $8Sm_2O_3$	c + t	c + t (trace)	c + t (small)
$98ZrO_2$ $2Gd_2O_3$	t	t	t
$95ZrO_2$ $5Gd_2O_3$	t + c	c + t	c + t
$92ZrO_2$ $8Gd_2O_3$	c + t (small)	c	c
$98ZrO_2$ $2Dy_2O_3$	t	t	t
$95ZrO_2$ $5Dy_2O_3$	t + c	c + t (small)	c + t (small)
$92ZrO_2$ $8Dy_2O_3$	c + t (trace)	c	c

Note: t = tetragonal, m = monoclinic, c = cubic, L = $cLa_2Zr_2O_7$, P = $cPr_2Zr_2O_7$, N = $cNd_{0.25}Zr_{0.75}O_{1.875}$. Heating rate = 1 °C min^{-1}, soaking time = 1 h. Ionic radius in 8-coordination (nm): Zr^{4+} = 0.0840, La^{3+} = 0.1160, Pr^{3+} = 0.1126, Nd^{3+} = 0.1109, Sm^{3+} = 0.1079, Gd^{3+} = 0.1053, Dy^{3+} = 0.1027.

The effect of size of the dopant cation on the crystallization behaviour of the fibres is clear from the above results. Thus, with relatively large cations lanthanum, praseodymium and neodymium as dopants, the products of calcination at 900 °C for all concentrations proved to be metastable t- and c-phases which changed to m-phase with or without an accompanying zirconate phase at higher temperatures. However, with the smaller ions samarium, gadolinium and dysprosium, the zirconates or the m-phase could not be detected under any conditions of this work, indicating better stabilization of the t- and c-phases (the latter at higher temperatures). Based on these essential differences, a tentative line is drawn between the two groups of cations, i.e. the large-sized lanthanum, praseodymium and neodymium (Group A cations) and the small-sized samarium, gadolinium and dysprosium (Group B cations). Table I compares the ionic sizes of the relevant cations.

3.2. Crystallite growth, lattice strain and grain growth

Variations in crystallite size of the different zirconia phases obtained at different temperatures of calcination (Table II) indicate not only the effects of dopant content and temperature, but also that of the size of the dopant cation (i.e. Group A or B). The basic observations are noted below.

TABLE II Crystallite sizes of the doped ZrO_2 fibres

Composition (mol %)	Temperature (°C)	Crystallite size (nm)
$98ZrO_2$ $2La_2O_3$	900	16.67 (t)
	1100	25.41 (t)
		16.42 (m)
	1300	33.65 (m)
$95ZrO_2$ $5La_2O_3$	900	16.94 (t/c)
	1100	27.46 (t)
		18.38 (L)
	1300	27.74 (m)
$92ZrO_2$ $8La_2O_3$	900	11.87 (c/t)
	1100	17.42 (t)
		16.02 (L)
	1300	N.D.[a]
$98ZrO_2$ $2Pr_2O_3$	900	16.49 (t)
	1100	31.41 (t)
		15.74 (m)
	1300	28.41 (m)
$95ZrO_2$ $5Pr_2O_3$	900	16.23 (t/c)
	1100	21.59 (t/c)
	1300	27.74 (m)
		27.79 (P)
$92ZrO_2$ $8Pr_2O_3$	900	12.45 (c/t)
	1100	15.27 (c/t)
	1300	23.30 (m)
		34.62 (P)
$98ZrO_2$ $2Nd_2O_3$	900	16.31 (t)
	1100	27.24 (t)
	1300	24.70 (m)
		27.24 (t)
$95ZrO_2$ $5Nd_2O_3$	900	15.46 (t/c)
	1100	24.83 (t/c)
	1300	37.13 (t)
$92ZrO_2$ $8Nd_2O_3$	900	10.79 (c/t)
	1100	20.65 (c/t)
	1300	29.58 (N)
		35.95 (t)
$98ZrO_2$ $2Sm_2O_3$	900	14.95 (t)
	1100	35.94 (t)
	1300	37.97 (t)
$95ZrO_2$ $5Sm_2O_3$	900	14.67 (t/c)
	1100	27.16 (t/c)
	1300	22.04 (t/c)
$92ZrO_2$ $8Sm_2O_3$	900	11.67 (c/t)
	1100	27.23 (c/t)
	1300	27.84 (c/t)
$98ZrO_2$ $2Gd_2O_3$	900	15.05 (t)
	1100	35.10 (t)
	1300	41.51 (t)
$95ZrO_2$ $5Gd_2O_3$	900	14.34 (t/c)
	1100	31.40 (c/t)
	1300	38.81 (c/t)
$92ZrO_2$ $8Gd_2O_3$	900	11.76 (c/t)
	1100	45.99 (c)
	1300	52.90 (c)
$98ZrO_2$ $2Dy_2O_3$	900	15.05 (t)
	1100	31.13 (t)
	1300	38.89 (t)
$95ZrO_2$ $5Dy_2O_3$	900	13.51 (t/c)
	1100	27.96 (c/t)
	1300	37.12 (c/t)
$92ZrO_2$ $8Dy_2O_3$	900	11.29 (c/t)
	1100	44.81 (c)
	1300	52.92 (c)

[a] N.D. = could not be determined.

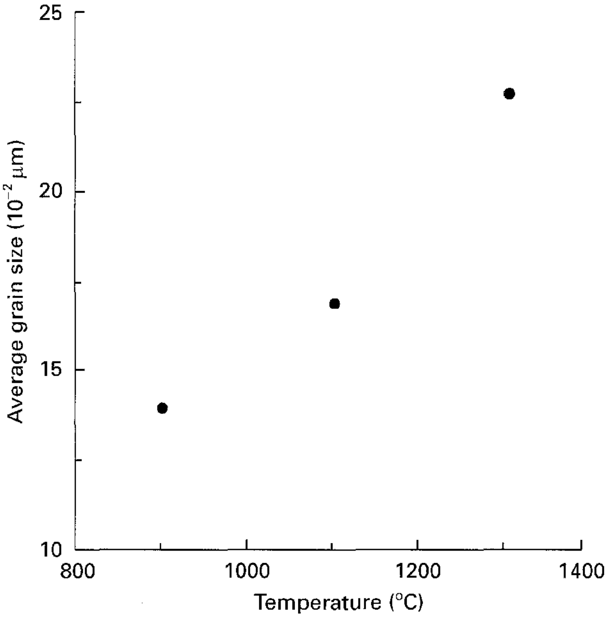

Figure 1 The change of average grain size with calcination temperature for $98ZrO_2$–$2Sm_2O_3$ fibres.

The fibres calcined at 900 °C showed a small decrease in crystallite size with increased content (2–8 mol % oxide) of any of the dopants [16]; no size effect of dopant cations was apparent. With increase in calcination temperature of fibres containing any percentage of Group B cations (giving rise to t- or c-phase or their combination) the crystallite size was found to increase drastically. The increase was especially significant for the transformation (t + c) → c, i.e. total conversion of t- to c-phase (again, for the two smallest cations). In case of Group A cations, a relatively small increase in crystallite size was noted with t → m transformation, and small decrease was evident for the t-phase with increase in dopant level.

The dramatic growth of the crystallites with increase in temperature for Group B cations, as mentioned above, was accompanied by a sharp decrease in lattice strain, which is an inherent feature of Equation 3. Thus, there was a general trend of decrease in lattice strain with increase in calcination temperature in all cases.

Crystallite size is also inversely related to surface area and energy, as shown by Garvie [17]. The conversion (t + c) → c, accompanied by a large increase in crystallite size and corresponding decrease in lattice strain, thus also indicates a significant decrease in surface energy, and hence, achievement of relative stability of the cubic structure with the given dopant contents.

As expected, the grain size of zirconia in calcined fibres increased with increasing calcination temperature in general. Fig. 1 shows data on the growth of t-ZrO_2 grains in, for example, 2 mol % Sm_2O_3-doped zirconia fibres as a function of calcination temperature. The microstructure of the fibres calcined at 1300 °C was found to be relatively dense, as shown in the fractured cross-section of one such fibre (Fig. 2).

3.3. Tensile strength

As in the case of hand-drawn sol–gel zirconia and zirconate-containing fibres of earlier work [6, 18], the tensile strength indicated a wide scatter, in spite of the

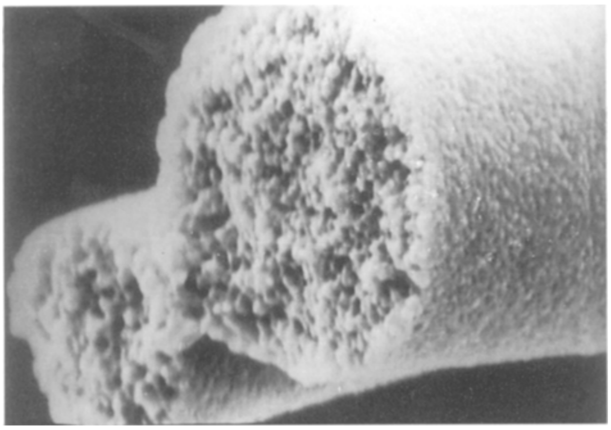

Figure 2 Scanning electron micrograph of $98ZrO_2$–$2Sm_2O_3$ fibres calcined at 1300 °C/1 h.

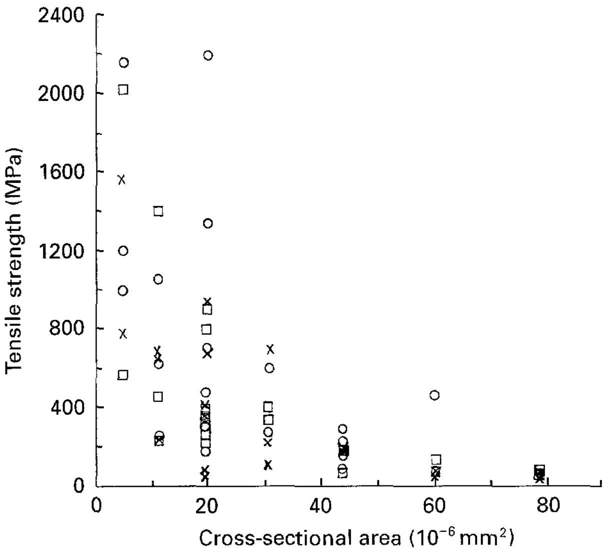

Figure 3 Variation of tensile strength with cross-sectional area of 2 mol % Ln_2O_3 (Ln = Sm, Gd, Dy) containing ZrO_2 fibres calcined at 1300 °C/1 h. (○) $98ZrO_2$ $2Dy_2O_3$, (□) $98ZrO_2$ $2Gd_2O_3$, (×) $98ZrO_2$ $2Sm_2O_3$.

fact that the present fibres were not hand-drawn but spun. There could be various reasons for this scatter, including incomplete densification (especially at 900 and 1100 °C), surface roughness and microcracks, defects due to sticking and bundling of gel fibres emerging from the spinneret, etc. A scatter plot for 2 mol % Group B oxide-doped fibres calcined at 1300 °C is presented in Fig. 3. A gradual fall in strength with increase in cross-sectional area [6] is evident in all cases, but a maximum strength of 1–2 GPa for the thinnest fibres [5, 6] is confirmed.

An interesting feature was that the maximum strength for 1300 °C calcined fibres decreased with increasing size of the dopant cation: 2.19, 2.01 and 1.55 GPa, respectively, for dysprosium, gadolinium and samarium; for the still larger neodymium, the fragility of the fibres prevented the measurement of their tensile strength. The same was true also for the other Group A cations, i.e. praseodymium and lanthanum. The case of Group A fibres is easily explained, as the fibres contained essentially the m-phase. In the case of Group B-containing fibres, the increase in maximum strength with decreasing dopant size is probably related to decreasing structural distortion of zirconia solid solution and increasing tendency of the cation to occupy Zr^{4+} sites in t-ZrO_2.

4. Conclusion

Zirconia fibres doped with 2–8 mol % oxide of lanthanum, praseodymium, neodymium, samarium, gadolinium and dysprosium were obtained by spinning acetate-derived sols and calcining them at 900, 1100 and 1300 °C. The nature of the calcined products divided the fibres into two groups: (a) those containing relatively large cations, i.e. lanthanum, praseodymium and neodymium (Group A) and yielding t-ZrO_2 at 900 °C but partly or fully m-ZrO_2 with or without a cubic zirconate phase at higher temperatures, and (b) those containing smaller cations, i.e. samarium, gadolinium and dysprosium (Group B), yielding only t-, c-, or (t- + c-) ZrO_2. This difference also caused differences in crystallite size, lattice strain and maximum tensile strength for 1300 °C calcined fibres. Although all the above cations are oversized compared to Zr^{4+}, such results indicate facile formation of m-ZrO_2 in the case of Group A cations and probably less structural distortion in c- and t-ZrO_2 in the case of Group B cations as dopants.

Acknowledgements

The authors thank Dr B.K. Sarkar, Director, for permission to publish this paper, and members of the Electro-Optic Section, for X-ray and SEM characterization of the fibres. Finally, the help and advice offered by colleagues of the Sol-Gel Laboratory, especially Drs Minati Chatterjee and Ramannan Venkatesh is acknowledged.

References

1. M. HAYASE, H. ASAMI, H. ASAKURA and T. SAEKI, *Shinagawa Tech. Rep.* **31** (1988) 129.
2. K. HATTORI and T. KURUSHIMA, *Ceram. Trans.* **31** (1993) 147.
3. E. LEROY, C. ROBIN-BROSSE and J. P. TORRE, in "Ceramics in Advanced Energy Technologies", edited by H. Krockel, M. Merz and O. Van der Biest (Reidel, Dordrecht, Holland, 1984) pp. 501–17.
4. K. KAMIYA, T. YOKO, K. TANAKA and H. ITOH, *Yogyo Kyokai-Shi* **95** (1987) 1157.
5. D. B. MARSHALL, F. F. LANGE and P. D. MORGAN, *J. Amer. Ceram. Soc.* **70** (1987) c–187.
6. K. KAMIYA, K. TAKAHASHI, T. MAEDA, H. NASU and T. YOKO, *J. Eur. Ceram. Soc.* **7** (1991) 295.
7. M. CHATTERJEE, A. CHATTERJEE and D. GANGULI, *Ceram. Int.* **18** (1992) 43.
8. W. PYDA, K. HABERKO and Z. ZUREK, *J. Eur. Ceram. Soc.* **10** (1992) 453.
9. T. LOG, R. A. CUTLER, J. F. JUE and A. V. VIRKAR, *J. Mater. Sci.* **28** (1993) 4503.
10. H. P. KLUG and L. E. ALEXANDER, "X-ray Diffraction Procedures for Polycrystalline and Amorphous Materials" (Wiley, New York, 1954) p. 491.
11. W. H. HALL, *Proc. Phys. Soc. Lond.* **62** (1949) 741.
12. I. H. COWDREY and R. G. ADAMS, "Materials Testing: Theory and Practice" (Wiley, New York, 1949) p. 17.

13. J. L. McCALL and W. M. MUELLER, "Microstructural Analysis: Tools and Techniques" (Plenum Press, London, 1973) pp. 42–8.
14. A. K. BHATTACHARYA, A. HARTRIDGE, K. K. MALLICK and J. L. WOODHEAD, *J. Mater. Sci.* **29** (1994) 6076.
15. R. A. McCAULEY, *J. Appl. Phys.* **51** (1980) 290.
16. J. L. SHI, Z. X. LIN and T. S. YEN, *J. Eur. Ceram. Soc.* **8** (1991) 117.
17. R. C. GARVIE, *J. Phys. Chem.* **69** (1965) 1238.
18. R. DAL MASCHIO, M. FILIPPONI, G. D. SORAJU, G. CARTURAN and G. M. DEL FELICE, *Bull. Amer. Ceram. Soc.* **71** (1992) 204.

Received 7 June 1995
and accepted 21 May 1996